Influence of pumice and fines contents on the extent of particle crushing in pumiceous sand-silt mixtures during undrained cyclic triaxial loading

Chaneva Jordanka [i)], Max O. Kluger [ii)], Vicki G. Moon [iii)], David J. Lowe [iv)] and Rolando P. Orense [v)]

i) Ph.D Student, School of Science, University of Waikato, Private Bag 3105, Hamilton 3240, New Zealand.
ii) Post-doctoral fellow, School of Science, University of Waikato, Private Bag 3105, Hamilton 3240, New Zealand.
iii) Senior - Lecturer, School of Science, University of Waikato, Private Bag 3105, Hamilton 3240, New Zealand.
iv) Professor, School of Science, University of Waikato, Hamilton 3240, New Zealand.
v) Professor, Department of Civil and Environmental Engineering, University of Auckland, Private Bag 92019 Auckland 1142, New Zealand.

ABSTRACT

Pumiceous particles have a distinct vesicular nature as well as a complex surface texture that makes them potentially vulnerable to crushing under cyclic loading. Pumiceous sand mixtures have received more scientific attention than pumiceous silts in this regard. Researchers have found the undrained cyclic behaviour of pumiceous sands to be significantly different from that of hard-grained sands because of the particle crushing that occurs during cyclic testing and/or sample reconstitution. The liquefaction resistance of pumiceous sands is also considered to be higher because of the pore-water pressure distribution in the sample that occurs during particle crushing. The undrained behaviour of pumiceous silt has only been studied once previously: such material did not crush during sample reconstitution and undrained cyclic testing, which was attributed to a cushioning effect taking place between silty, non-crushable particles and coarse sandy pumice particles. Whether there are thresholds of fines content and/or pumice content at which pumiceous soil mixtures start to behave more similarly to hard-grained soils are yet to be unravelled and remain relevant for engineers and scientists. This paper analyses particle crushing after sample reconstitution and undrained cyclic triaxial testing of three pumiceous natural soil mixtures (lacustrine tephra deposits) from northern New Zealand having fines (< 0.075mm) and pumice contents ranging between 20% and 70% and 30% and 51%, respectively. The results examine potential changes in (1) fines content, (2) pumice content, and (3) undrained cyclic behaviour by comparing both pore-water pressure and axial strain development of the pumiceous soils with other crushable and non-crushable soils.

Keywords: pumiceous sand-silt mixtures, particle crushing, pumice content, fines content, cyclic triaxial testing

1 INTRODUCTION

Pumiceous particles are vesicular, volcanic-ash soils that are characterised by a "foam-like", lightweight structure with high angularity, making them particularly vulnerable to crushing compared to hard-grained, quartzitic soils. The occurrence of particle crushing in pumiceous sands under undrained cyclic loading has been considered the main reason for the differences in (1) undrained cyclic behaviour and (2) liquefaction resistance of pumiceous sands compared with hard-grained sands (Hyodo et al., 1998; Orense et al., 2012; Asadi et al., 2018). The above-mentioned studies discussed results for natural pumiceous sands containing both pumiceous and hard-grained (mostly quartzitic) particles. Whether the amount of pumice particles (i.e., pumice content) could be a relevant parameter influencing the extent of particle crushing, and thus the undrained cyclic behaviour and liquefaction resistance, is still an open question. Asadi et al. (2018) analysed the different levels of particle crushing of three different natural pumiceous mixtures with fines content (percentage of particles finer than 0.075mm) varying between 0 and 13%. They inferred that the different levels of particle crushing of the sands could have been caused by the different pumice contents. Stringer (2022) tested undisturbed pumiceous sand samples and found that major changes in liquefaction resistance occurred at relatively low pumice contents, suggesting that the effect of particle crushing can be present even in sands with low pumice content. To what extent the findings for pumiceous sands extend to pumiceous silts remains unknown. Until the present time, the research focus related to particle crushing during undrained cyclic testing has been almost exclusively on pumiceous sands and information about pumiceous materials dominated by silt and silty sand is scarce. A study about the undrained behaviour and liquefaction resistance of pumiceous sandy silt (51.2% fines) found the undrained cyclic behaviour of the silty material to be more similar to that of hard-grained soils than to that of pumiceous sands (Chaneva et al., 2023). The reason considered was

that the high amount of fines acted as cushions between the sandy particles, thereby preventing significant particle crushing. Identifying the thresholds of both pumice and fines contents at which particle crushing becomes relevant is important to both geotechnical practitioners and researchers.

This paper investigates the particle crushing under undrained cyclic triaxial testing of three pumiceous soil materials with different pumice contents, ranging from 30 to 51%, and different fines content, ranging from 20 to 70%. All three materials are natural rhyolitic volcanic-ash (tephra fall) materials deposited in lakes. The extent of particle crushing is quantified and presented from three perspectives: (1) change in grain size distribution after testing; (2) change in pumice content after testing; and (3) change in undrained cyclic behaviour after testing (through the pore water pressure and double axial strain development). The results from (1) and (2) are compared with the pumice content and fines content of the virgin (original) materials.

2 METHODS AND MATERIALS

2.1 Sampling location and procedure

The soil materials examined are derived from one rhyolitic pumiceous layer, Mamaku tephra, sampled at the shore of Lake Areare (Fig. 1a.), which is located in the Hamilton lowlands in the North Island of New Zealand. The Mamaku tephra layer (deposited ~8.0 cal ka) is one of many lacustrine pumiceous layers deposited in the area, which have liquefied due to earthquakes in the past ~17.5 cal ka (Kluger et al., 2023). At Lake Areare, the Mamaku tephra layer occurs in the exposed lake bed at a relatively shallow sediment depth of <0.5 m. In order to obtain the material, a large number of small block samples (each with a volume of ~0.0075 m^3) containing the ~2 cm-thick Mamaku tephra layer were sampled. The Mamaku tephra lies a few centimetres below the ~7.6 cal ka-aged Tuhua tephra layer (Kluger et al., 2023) and both tephras are encapsulated by organic lake sediments. The Mamaku tephra layer contains three different sublayers, or beds, of different grain size distributions. The three beds have thicknesses (from the top) of ~1 cm, ~0.3 cm, and ~0.7 cm. Once in the lab, the beds were carefully sampled using a spoon after being cleaned from organic contamination and oven dried at 40°C.

2.2 Sample properties

Relevant physical and geotechnical properties for the three beds in the Mamaku tephra layer were obtained to accompany the triaxial testing, including grain size distribution, particle density, minimum and maximum dry density, Atterberg limits, and pumice content.

The grain size distributions were obtained before (i.e., virgin soils) and after testing (i.e., after reconstitution, consolidation, and shearing) on small-volume samples using laser diffraction analysis with a Malvern Mastersizer 3000 apparatus.

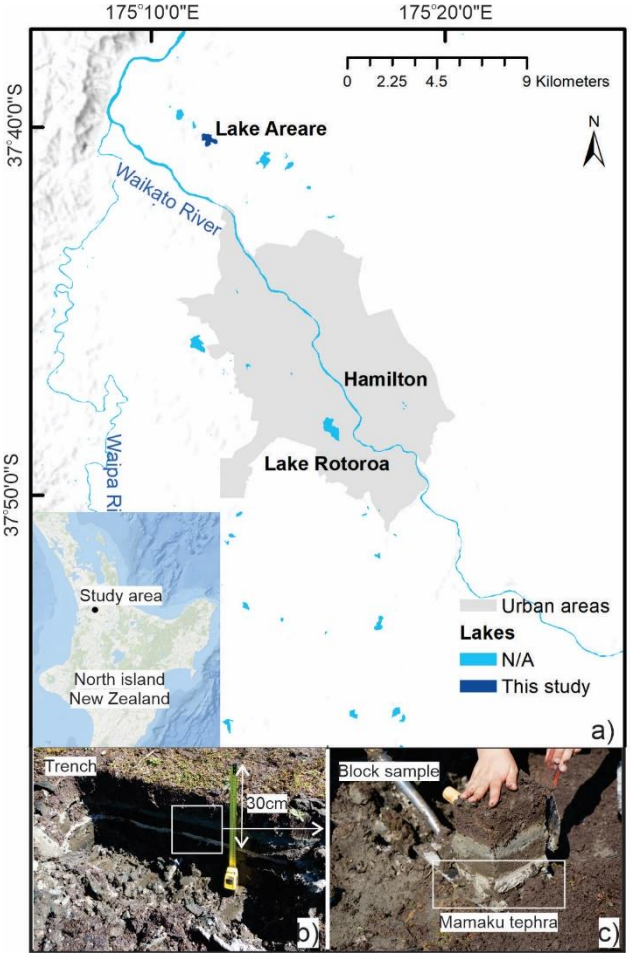

Fig. 1. (a) Location of the sampling area for Mamaku tephra at Lake Areare in the Hamilton lowlands and faults in the area, North Island, New Zealand; (b) shallow trench where the blocks were sampled; and (c) block samples containing Mamaku tephra (cream-coloured lower layer).

The particle density was determined using a Quantachrome Ultrapyc 1000 nitrogen-filled gas pycnometer following ASTM-D5550-14 (ASTM, 2014). Minimum and maximum dry densities of the samples were obtained following the Japanese standard method (JGS, 2009) as modified by Mijic et al. (2021). Atterberg limits were obtained following ASTM-D4318-00 (ASTM, 2017). Scanning electron microscopy (SEM) was undertaken using a Hitachi S-4700 FE SEM. SEM images of components of the three beds of Mamaku tephra are presented in Figure 2.

The pumice content was estimated using a point-counting method (Frolov and Maling, 1969). Four SEM images of representative grain clusters were chosen for each sample and were counted systematically on crossing points (150 points per image) of rectangular grids.

The top bed of Mamaku tephra, with 70% fines content, tested as non-plastic and will be referred to as Ma-ML70 hereafter (low plasticity silt, with 70% fines).

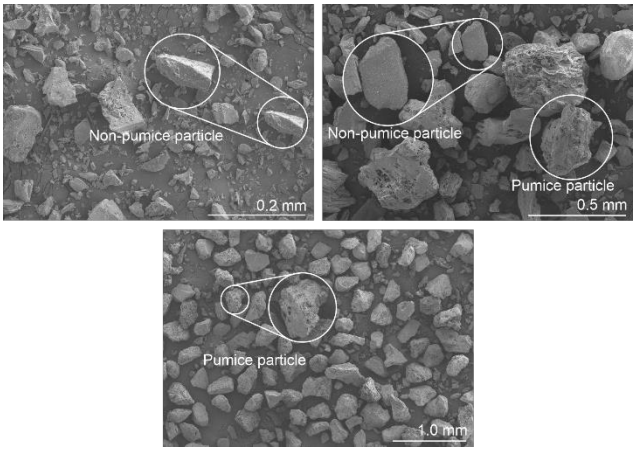

Fig. 2. SEM images of Ma-ML70 (top left), Ma-SM31(top right), and Ma-SM20 (bottom middle).

The middle and bottom beds of the Mamaku tephra layer were classified as sandy silts with 20% and 31% fines contents, respectively, and will be referred to as Ma-SM20 and Ma-SM31, respectively. The specific gravity G_s, mean diameter D_{50}, pumice content PC, and minimum and maximum void ratios e_{min} and e_{max}, are summarized in Table 1. The grain size distribution curves of the virgin materials are presented in Fig. 3.

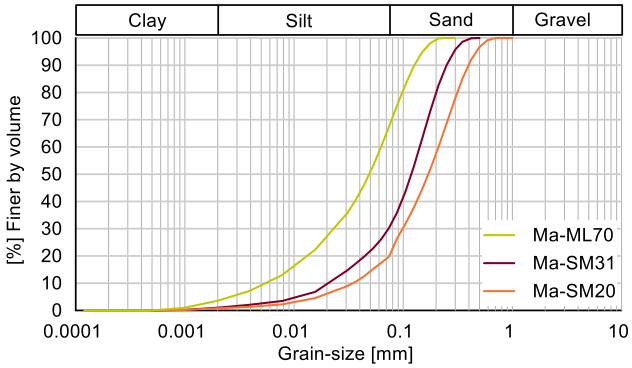

Fig. 3. Grain size distribution of virgin (before testing) pumiceous soil materials (beds of Mamaku tephra).

Table 1. Index properties of materials

	G_s	D_{50} (mm)	FC (%)	PC (%)	e_{min}	e_{max}
Ma-ML70	2.41	0.049	70	30±11	0.88	2.07
Ma-SM31	2.40	0.118	31	50±10	0.69	1.5
Ma-SM20	2.40	0.169	20	51±8	0.7	1.28

2.3 Triaxial testing

A GDS advanced dynamic triaxial testing system was used for the triaxial testing of the samples. The samples, with a target size of 50 mm in diameter and 100 mm in height, were reconstituted using the under-compaction method following the procedure of Ladd (1978). Samples with 15% water content were reconstituted in eight layers into a split mould mounted on top of the triaxial base plate. Saturation pressures of at least 800 kPa were applied over 15 h to the samples. When the B-value of more than 0.95 was reached, the samples were considered to be saturated. Samples were tested at effective consolidation stresses of 20 and 100 kPa. The low consolidation stress was chosen because it best corresponded to the in-situ vertical stress of the Mamaku tephra, and the higher consolidation stress was used to enable direct comparison of the test results with those for other materials found in the literature.

The target relative densities were chosen so that a wide range of densities was covered. The sands were reconstituted within the lower range of medium-high density (as per Terzaghi and Peck, 1967), and the silt was reconstituted in the higher range of medium to high densities.

A total of 21 cyclic tests were performed. The cyclic stress amplitudes were applied with a frequency of f = 0.02 Hz. The initiation of cyclic liquefaction, according to ASTM D 5311 - 92, was considered. The CSR (Cyclic Stress Ratio) range for all the presented tests was 0.06–0.18.

3 RESULTS

3.1 Grain size distribution

The change in grain size distributions after cyclic triaxial testing is presented by observing the changes in the D_{10}, D_{50}, and D_{90} grain-size parameters (Fig. 4). Firstly, by analysing all the data points for the three Mamaku materials, it can be observed that there are no noticeable trends when considering the different consolidation stresses. The scatter in the data points implies that the consolidation stress did not affect any potential particle crushing of the samples.

Ma-ML70 samples (yellow-coloured data points), with fines content and pumice content of 70% and 30%, respectively, were only tested at a relative density (Dr_c) of ~0.8, and the grain size parameters after testing are similar to those of the virgin material (indicated by dashed lines). Therefore, we infer that no crushing has occurred within the full range of testing conditions (different consolidation stresses and cyclic stress amplitudes) for this pumiceous silt. Considering that Ma-ML70 did not show signs of crushing at a high relative density, it is expected that it would not crush at lower densities either.

The Ma-SM31 samples (red data points), with fines content and pumice content of 31% and 50%, respectively, were reconstituted under a relative density of ~0.6. The grain size parameters D_{10} and D_{50}, after testing, exhibit a slight positive offset from those values obtained from the virgin material, whereas no significant difference was observed in D_{90}. Thus, the results imply a slight decrease in the silt to very fine sand grain size fractions. Note that the relative density of ~0.6 was the highest density that the samples could have been reconstituted using gentle moist tamping.

The Ma-SM20 samples (orange data points), with fines content and pumice content of 20% and 51%, respectively, were tested under two relative densities

(~0.4 and ~0.6) and two consolidation stresses.

The grain size parameters of samples with lower relative density (~0.4) all systematically plot beneath those of the virgin material, being especially evident for D_{50} and D_{90} values. The negative offset in grain size parameters is even more noticeable for the samples reconstituted at the higher density (~0.6), indicating that particles have crushed significantly and hence highlighting the effect of the relative density in the extent of particle crushing.

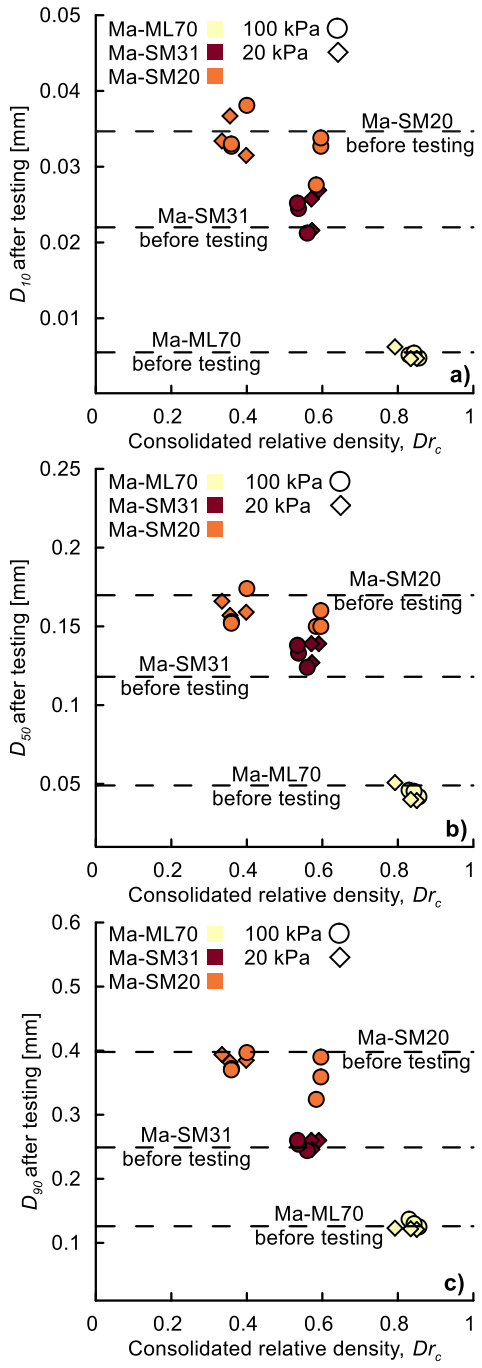

Fig. 4. Grain size parameters (a) D_{10}, (b) D_{50} and (c) D_{90} for virgin Mamaku tephra samples (of the three beds) before and after testing.

The grain size distribution results for Ma-SM20 suggest that particle crushing occurred after testing the sand under the range of applied testing conditions.

3.2 Pumice content

The change in pumice content before and after testing was considered under the hypothesis that fewer pumiceous particles after testing would indicate particle crushing because the pumiceous particles, especially in the fine and medium sand size range, would break down down into glass shards – which are considered non-pumice. Note that the definition of non-pumice particles can be different for different pumiceous soil mixtures and, in this study, non-pumiceous particles are glass shard particles. The pumice content of the samples after testing, as well as the original pumice content of the Mamaku tephra materials, are plotted in Fig. 5.

The coloured data points represent the pumice contents of the Mamaku materials after triaxial testing, together with their corresponding standard deviations, *SD* (vertical error bars).

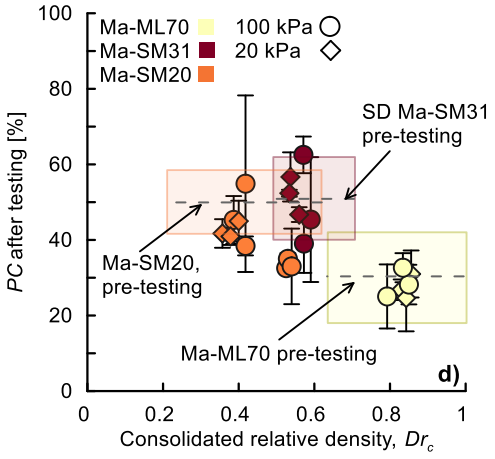

Fig. 5. Pumice content for virgin Mamaku tephra sample materials (the three beds) before and after testing.

The dashed horizontal lines represent the virgin materials' pumice contents, and the coloured squares represent the standard deviations of the virgin materials' pumice content values.

The pumice contents of Ma-ML70 and Ma-SM31 materials obtained after testing mostly lay within the standard deviations of the equivalent virgin materials, indicating that the pumice contents of those materials did not significantly change, and, therefore, no crushing occurred due to triaxial testing at the consolidation stresses and relative densities considered.

The pumice contents of Ma-SM20 (orange data points) obtained after triaxial testing lie below the standard deviation of the equivalent virgin material, suggesting that particle crushing took place for this particular pumiceous sand, with it being most evident for the denser samples (Dr_c~0.55).

3.3 Cyclic undrained behaviour

The normalised axial strain development and pore-water pressure development plots are presented in Fig. 6. The full line curves (yellow, red and orange) are median curves of the results from the three different Mamaku beds.

For discussion purposes, results from the studies of Asadi et al. (2018) and Chaneva et al. (2023) are plotted as well (Fig. 6). The dark green and grey zones (zones A and B) correspond to ranges typical for pumice sand (with a relative density of ~0.8) and hard-grained Toyoura sand (with a relative density of ~0.5), respectively, as per Asadi et al. (2018). The dashed black curve is a median curve taken from the results for the pumiceous silt (51% fines and 48% pumice content) from Chaneva et al. (2023).

In their study, Asadi et al. (2018) found that the cyclic behaviour of pumiceous sands is characterised by a gradual increase in axial strain until liquefaction occurs. Pumice sand exhibits a pronounced pore-water pressure accumulation at the beginning of undrained cyclic loading, reaching high values of $r_u > 0.8$, well before liquefaction is initiated. In contrast, hard-grained Toyoura sand typically exhibits a more stable undrained cyclic behaviour with pronounced axial strain and pore-water pressure increases limited to the final phase of the undrained cyclic loading. The differences in undrained cyclic behaviour were attributed to the crushing of the pumice particles that we argued to be largely dependent on the relative density and was most evident for samples with a high relative density, e.g., ~0.8. In the study by Chaneva et al. (2023), it was found that pumiceous silt with 51% fines and 48% pumice content was not crushable, and the undrained cyclic behaviour was similar to that of hard-grained sands.

If we consider the zones of the results for the pumice sand and the hard-grained sand from Asadi et al.'s study to be the boundaries between crushable and non-crushable undrained soil behaviour trends, we can discuss the results for the Mamaku tephra materials in a particle crushing manner. Note that other soil or particle properties that affect the undrained soil behaviour, such as particle shape and angularity, are not considered in the discussion. The different testing conditions, such as consolidation stress, density and cyclic stress ratios, are not discussed separately. Instead, a trend that considers the different soils by means of grain size and pumice content alone is observed. The Mamaku results, shown by analyses of samples Ma-ML70, Ma-SM31, and Ma-SM20, are presented with a single median curve per material.

The yellow line presents the median curve for all the Ma-ML70 tests and clearly plots closest to the hard-grained (i.e., non-crushable) Toyoura sand. Ma-SM20 is presented with the orange line, and it plots the closest to the natural crushable pumice zone published by Asadi et al. (2018). The results from the undrained cyclic behaviour tests for Ma-SM31 (red line) plot in the middle, between those for Ma-SM20 and Ma-ML70.

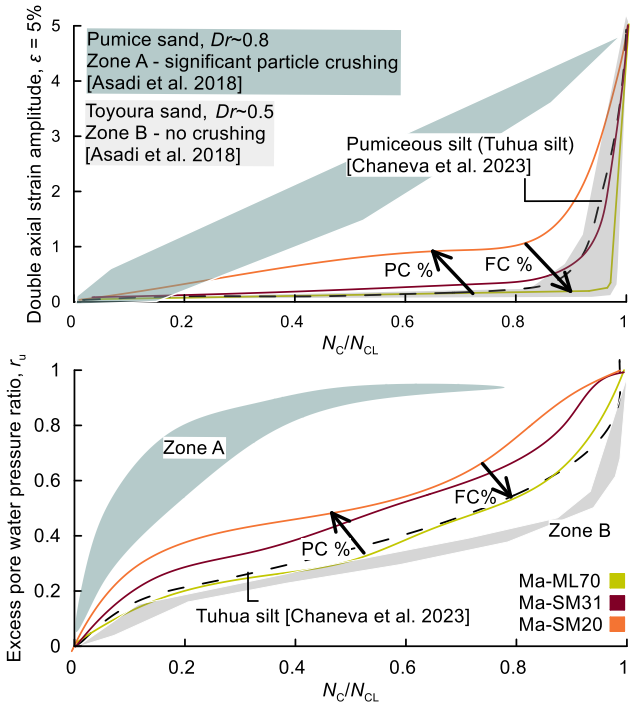

Fig. 6. Normalised axial strain and pore pressure development median curves for Ma-ML70, Ma-SM31, and Ma-SM20 (yellow, red and orange lines, respectively) plotted against relevant results (zones and median curves) from published literature.

The results for the three Mamaku materials show a clear trend based on the fines contents of the virgin soils. Namely, the coarser the soil particles are, the closer the results plot to the pumice crushable sand zone, indicating higher crushability. Moreover, the results for the pumiceous silt from Chaneva et al. (2023) (with fines content of 51%) also fall into the trend with the median curve of the silt (51% fines), plotting in between the Ma-ML70 and Ma-SM31.

Considering the fact that the pumice contents of Ma-SM31 and Ma-SM20 are relatively similar (50% and 51%, respectively) to the pumiceous silt (48%) from Chaneva et al. (2023), a pumice content-based trend is less conclusive. Yet, sample Ma-ML70 (the Mamaku tephra bed with the lowest pumice content) plots closest to the hard-grained Toyoura sand zone (zone B), and sample SM20, with the highest pumice content (51%), plots closest to the Pumice sand zone (A), and so a subtle trend can be observed. Soil materials that cover a wider range of pumice content values should be tested in order to further investigate whether there is a threshold of pumice content upon which particle crushing starts.

5 CONCLUSIONS

Particle crushing of three tephra-derived pumiceous silt materials, Ma-ML70, Ma-SM31, and Ma-SM20, with different pumice and fines contents, based on 21

undrained triaxial cyclic tests, was analysed and evaluated. Observations based on grain size distribution, pumice content changes, and cyclic undrained behaviour allowed us to make the following conclusions:

(1) No change in grain size nor pumice content was observed for the silty Mamaku Ma-ML70. Moreover, the cyclic behaviour, by means of pore pressure distribution as well as double axial strain accumulation of Ma-ML70, is similar to that of hard-grained sands and non-crushable silts from the literature, indicating no particle crushing occurred.

(2) The silty Mamaku sand sample with 31% fines, Ma-SM31, showed no changes in grain size as well as pumice content after testing. The results from the undrained cyclic testing do not resemble the typical crushable trends. The results for this pumiceous material also indicate that no particle crushing occurred during the cyclic testing.

(3) For the coarsest Mamaku sand, with 20% fines, Ma-SM20, both for the grain size and the pumice content, changes indicating particle crushing were evident. The undrained cyclic behaviour results plot the closest to the crushable zone based on published data, compared to the other two Mamaku materials. Thus, it can be inferred that Ma-SM21 underwent particle crushing for the used testing condition.

(4) Considering the crushing results and the fines contents of the three materials as well as the available published data on pure pumiceous sand and a pumiceous (51% fines content) silt, if a fines threshold where particles begin to crush under cyclic triaxial testing is to be speculated, it would be in between 31% and 20%.

(5) Considering the fact that Ma-SM20 sand with a 50% pumice content is crushable, and that there are published data for pumiceous silt with 48% pumice content proven not to be crushable, a definitive conclusion based on the effect of pumice content alone cannot yet be made.

ACKNOWLEDGEMENTS

We acknowledge funding support as follows: the MBIE Endeavour Fund (Smart Ideas) contract UOWX1903; the Marsden Fund contract UOW1902; the New Zealand Centre for Earthquake Resilience (QuakeCoRE); the Earthquake Commission Toka Tū Ake EQC (Contract BIG 012 2020); and Waikato Regional Council (support for project on paleoseismicity and liquefaction). We thank Richard Melchert, Tehnuka Ilanko, Tom Robertson, Ben Roche, Helen Turner, and Vittoria Gibbons for help in the field and/or lab, and Mrs Hekeiterangi Broadhurst (Kuia Kaumatua) and Wiremu Puke of Ngāti Wairere (Hukanui Marae), Waikato District Council, and the Department of Conservation, for supporting access to Lake Areare.

REFERENCES

1) Asadi, M. S. et al. (2018): Undrained cyclic behavior of reconstituted natural pumiceous sands. *Journal of Geotechnical and Geoenvironmental Engineering*, 144(8), 434–441. doi: 10.1061/(ASCE)GT.1943-5606.0001912.
2) ASTM-D-2487 (2018): Classification of soils for engineering purposes (USCS). *American Society for Testing and Materials*.
3) ASTM-D4318-17e1 (2017): Standard test methods for liquid limit, plastic limit and plasticity index of soils. American Society for Testing and Materials.
4) ASTM-D5550-14 (2014): Standard test methods for specific gravity of soil solids by water pycnometer. American Society for Testing and Materials.
5) ASTM D 5311 - 92 (2004): Standard test method for load controlled cyclic triaxial strength of soil., American Society for Testing and Materials. doi: 10.1520/D5311-11.2.
6) Chaneva, J. et al. (2023): Monotonic and cyclic undrained behaviour and liquefaction resistance of pumiceous, non-plastic sandy silt. Soil Dynamics and Earthquake Engineering, 168(December 2022), 107825. doi: 10.1016/j.soildyn.2023.107825.
7) Frolov, Y. S. and Maling, D. H. (1969): The accuracy of area measurement by point counting techniques. Cartographic Journal, 6(1), 21–35. doi: 10.1179/caj.1969.6.1.21.
8) Hyodo, M., Hyde, A. F. L. and Aramaki, N. (1998): Liquefaction of crushable soils. Geotechnique, 48(4), 527–543. doi: 10.1680/geot.1998.48.4.527.
9) Japanese Geotechnical Society (2009): Standard, J.-2009: Test method for minimum and maximum densities of sand.
10) Kluger, M. O. et al. (2023): Seismically-induced down-sagging structures in tephra layers (tephra-seismites) preserved in lakes since 17.5 cal ka, Hamilton lowlands, New Zealand. Sedimentary Geology, 445, (106327), 1–22. doi: https://doi.org/10.1016/j.sedgeo.2022.106327.
11) Ladd, R. S. (1978): Preparing test specimens using undercompaction. Geotechnical Testing Journal, 1(1), 16–23.
12) Mijic, Z. et al. (2021): Test method for minimum and maximum densities of small quantities of soil. Soils and Foundations, 61(2), 533–540. doi:0.1016/j.sandf.2020.12.003.
13) Orense, R. P., Pender, M. J. and O'Sullivan, A S. (2012): Liquefaction characteristics of pumice sands. EQC Project.
14) Stringer, M. (2022): Response of pumice-rich soils to cyclic loading. Proc., 4th International Conference on Performance Based Design in Earthquake Geotechnical Engineering, 530–544.
15) Terzaghi, K. and Peck, R. B. (1967): Soil Mechanics in Engineering Practice. 2nd ed. Wiley International, NY.